Cytokine 123 (2019) 154760

Contents lists available at ScienceDirect

Cytokine

journal homepage: www.elsevier.com/locate/cytokine

In vivo and in vitro anti-inflammatory and pro-osteogenic effects of citrus cystatin *Csin*CPI-2

Natalia Da Ponte Leguizamón[a,1], Elisandra Marcia Rodrigues[b,1], Michel Leandro de Campos[c], Andressa Vilas Boas Nogueira[a], Kennia Scapin Viola[b], Vanessa Karine Schneider[d], Daniela Morilha Neo-Justino[d], Mario Tanomaru-Filho[b], Willian Fernando Zambuzzi[e], Flavio Henrique-Silva[d], Andrea Soares-Costa[d], Gisele Faria[b,*], Joni Augusto Cirelli[a,*]

[a] Department of Diagnosis and Surgery, School of Dentistry at Araraquara, Sao Paulo State University – UNESP, Araraquara, São Paulo, Brazil
[b] Department of Restorative Dentistry, School of Dentistry at Araraquara, Sao Paulo State University – UNESP, Araraquara, São Paulo, Brazil
[c] Health Sciences Institute, Federal University of Mato Grosso – UFMT, Sinop, Mato Grosso State, Brazil
[d] Department of Genetic and Evolution, Federal University of Sao Carlos, São Carlos, Brazil
[e] Department of Chemistry and Biochemistry, Laboratory of Bioassays and Cell Dynamics, Institute of Biosciences, Sao Paulo State University – UNESP, Botucatu, São Paulo, Brazil

ARTICLE INFO

Keywords:
Cystatins
Cysteine proteinases
Cytokines
Cathepsins

ABSTRACT

Cystatins are natural inhibitors of cysteine peptidases. Recently, cystatins derived from plants, named phytocystatins, have been extensively studied. Among them, *Csin*CPI-2 proteins from *Citrus sinensis* were identified and recombinantly produced by our group. Thus, this study described the recombinant expression, purification, and inhibitory activity of this new phytocystatin against human cathepsins K and B and assessed the anti-inflammatory effect of *Csin*CPI-2 in vitro in mouse and in vivo in rats. In addition, the pro-osteogenic effect of *Csin*CPI-2 was investigated in vitro. The inflammatory response of mouse macrophage cells stimulated with *P. gingivalis* was modulated by *Csin*CPI-2. The in vitro results showed an inhibitory effect ($p < 0.05$) on cathepsin K, cathepsin B, IL-1β, and TNF-α gene expression. In addition, *Csin*CPI-2 significantly inhibited in vivo the activity of TNF-α ($p < 0.05$) in the blood of rats, previously stimulated by *E. coli* lipopolysaccharide (LPS). *Csin*CPI-2 had a pro-osteogenic effect in human dental pulp cells, demonstrated by the increase in alkaline phosphatase (ALP) activity, deposition of mineralized nodules, and the gene expression of the osteogenic markers as bone morphogenetic protein 2 (BMP-2), runt-related transcription factor 2 (Runx-2), ALP, osteocalcin, and bone sialoprotein (BSP). These preliminary studies suggested that *Csin*CPI-2 has a potential anti-inflammatory, and at the same time, a pro-osteogenic effect. This may lead to new therapies for the control of diseases where inflammation plays a key role, such as periodontal disease and apical periodontitis.

1. Introduction

Immune-inflammatory processes involve a cascade of events triggered by cellular mediators, mainly cytokines [1], which are the key molecules in acute and chronic inflammation [2]. In this scenario, enzymes, such as cysteine peptidases (CPs), are also important molecules that degrade components of the host tissue. Under pathological conditions, the interplay between molecules such as cytokines, cysteine peptidases, and their inhibitors cystatins, promote the onset and progression of diseases associated with bone loss such us osteoarthritis, rheumatoid arthritis, and periodontal disease [3].

Lysosomal cysteine cathepsins are a family of cysteine peptidases which play an important role in bone resorption [4,5]. One of them, cathepsin K (CTSK), is the major CP involved in bone resorption; it is predominantly expressed in osteoclasts, and it is induced in osteoclast differentiation [5,6]. CTKS is considered an important target for the treatment of different bone diseases [7]. In vivo studies in mice showed that CTSK gene deletion or silencing prevented bone loss through the

* Corresponding authors at: Department of Diagnosis and Surgery, School of Dentistry at Araraquara, São Paulo State University, Rua Humaitá, 1680, Centro, 14801-903 Araraquara-SP, Brazil. (J.A. Cirelli). Department of Restorative Dentistry, School of Dentistry at Araraquara, São Paulo State University, Rua Humaitá, 1680, Centro, 14801-903 Araraquara-SP, Brazil. (G. Faria).
E-mail addresses: gisele.faria@unesp.br (G. Faria), joni.cirelli@unesp.br (J.A. Cirelli).
[1] These authors contributed equally to this study.

https://doi.org/10.1016/j.cyto.2019.154760
Received 21 November 2018; Received in revised form 6 June 2019; Accepted 10 June 2019
Available online 18 June 2019

reduction of osteoclast function and modulated the immune response in experimental periodontitis and rheumatoid arthritis models [6,8].

Another CP involved in inflammatory diseases and pathological processes is cathepsin B (CTSB) [9]. This enzyme participates in the degradation of intracellular proteins and the components of the extracellular matrix [10]. CTSB is also involved in various cellular processes including cancer metastasis, myoblast differentiation, interleukin-1 (IL-1) production, cell death, and it also mediates inflammation, since it is necessary for tumor necrosis factor-alpha (TNF-α) and the secretion of other pro-inflammatory cytokines, such as IL-1, IL-2, IL-6, and IL-8 [9,11,12]. In an in vitro study, CTSB inhibition reduced the production of cytokines and showed anti-inflammatory activity in mouse macrophage cells stimulated by lipopolysaccharide [9].

Proteinaceous cysteine peptidase inhibitors are designated as cystatin, an emerging class of drugs that are potent antagonists of osteoclast activity [13]. Cystatins has been used due to its ability to inhibit CTSK and CTSB activity, and its use leads to reduced bone loss in the osteoporosis process [14].

Cystatins are tight-binding competitive inhibitors that block the proteolytic activity of cysteine proteinases [15]. Mammalian cystatins are grouped into 3 family types; they are present in the human body distributed in tissues and fluids [16,17].

The treatment of mouse bone marrow-derived cells in vitro and calvarial cells in vivo with Cys C induced a high level of expression of bone morphogenetic protein 2 (BMP-2) and run-related transcription factor (2Runx-2) mRNA expression; important molecules involved in osteogenesis [18]. Furthermore, stimulated Cys C increased alkaline phosphatase (ALP) activity, the mineralization of the new bone matrix, and calvarial bone formation [18]. Another Cystatin, Cys B, inhibits bone resorption in rat osteoclasts by down-regulating intracellular Ctsk activity [6].

Phytocystatins are cystatins derived from plants, and they are involved in plant development and in response to biotic and abiotic stresses. [19,20]. Among them, cystatins derived from sugarcane, named CaneCPI-1 (canecystatin) [21], CaneCPI-2, CaneCPI-3 [22], CaneCPI-4 [23,24], and CaneCPI-5 have been studied [25]. The first study showing the inhibitory activity of these phytocystatins on CTSK, CTSL, and CTSB was reported by Oliva et al. [26]. Later, the inhibitory effect of canecystatin was demonstrated on human CTSB and CTSL when canecystatin CaneCPI-4 inhibited the invasive ability of human breast cancer cells [23]. More recently, a gene sequence encoding a new phytocystatin named *Csin*CPI-2 from *Citrus sinensis* was cloned into the eukaryotic expression vector pET28a (Novagen, Madison, WI, USA), and was overexpressed in *E. coli* cells. Thus, the aim of this study was to describe the expression, purification, and inhibitory activity of this new phytocystatin (CsinCPI-2), identified in *Citrus sinensis*, and to assess the anti-inflammatory effect of this protein, combining in vitro in mouse macrophage cells and in vivo rats experiments. In addition, a pro-osteogenic effect of *Csin*CPI-2 was investigated in vitro (human dental pulp cells).

2. Materials and methods

2.1. CsinCPI-2 cloning and recombinant expression in E. coli cells

Citrus sinensis cystatin, *Csin*CPI-2, was identified from the Phytozome v 12.1 database [27] using the word "cystatin." The signal peptide prediction analysis was performed using SignalP version 4.1 [28], protein features, such as molecular mass and isoelectric point (pI), were obtained using the ProtParam software [29]. The comparative alignment to motif evaluation and similarity between *Csin*CPI-2 and other phytocystatins (that present a higher identity with *Csin*CPI-2 protein with blastp tool analysis [30]) was made using the Multalin program [31], with parameters of a maximum consensus value of 90% and a minimum consensus value of 50%.

The coding region of 312 bp cystatin from *Citrus sinensis*, named *Csin*CPI-2 (orange1.1g034261m - Phytozome) was synthetically synthesized using the Epoch gene (Epoch Life Science, Missouri, TX, USA) and cloned into a pBSK plasmid. The fragment of interest was isolated with *Nde* I and *Eco* RI restriction enzymes, and cloned into expression vector pET28a (Novagen, Madison, WI, USA) cut with the same enzymes, in frame, with a His-tag coding sequence. pET28a*Csin*CPI-2 was sequenced in a MegaBACE 1000 Flexible Sequencer (GE Healthcare, Chicago, IL, UK) using a DYEnamic ET Dye Terminator Kit (GE Healthcare). Recombinant expression and purification were performed as described [21]. Briefly, the expression vector, pET28aCsinCPI-2, was used to transform the cells of *E. coli* Rosetta (DE3) to calcium chloride components. The transformed cells were cultivated overnight at 37 °C in 50 ml of a selective medium containing kanamycin and chloramphenicol antibiotics (25 μg/ml) under agitation at 200 rpm. After that, 5 ml of the culture was transferred to 500 ml of medium containing antibiotics, this culture was cultivated until it reached an optical density (O.D.) of 0.6 at 600 nm when the protein expression was induced by the addition of IPTG at a final concentration of 0.4 mM. After induction, the cells were collected, centrifuged, and resuspended in 10 ml of lysing buffer (10 mM Tris–HCl, 100 mM NaCl, and 50 mM NaH_2PO_4, pH 8.0), the cells were disrupted by sonication five times for 1 min at 30 s intervals. The lysate was centrifuged at 13,000*g* at 4 °C for 10 min, and the supernatant and precipitate were analyzed in 15% SDS–PAGE. The His-tagged recombinant protein was purified from the supernatant using affinity chromatography with Ni-NTA agarose protein (Qiagen Hilden, NRW, DE), it was then eluted with the same buffer containing increasing imidazole concentrations (10, 25, 50, 75, 100, and 250 mM). The fractions containing the purified protein were pooled and dialyzed against phosphate-buffered saline (PBS) at a pH of 7.4. The protein concentration was determined using a Pierce BCA Protein Assay Kit (Thermo Fisher Scientific, Waltham, MA, USA).

2.2. Inhibition of cathepsin activity

Human CTSK (EC 3.4.22.38, Sigma-Aldrich) and human CTSB (EC 3.4.22.1, R&D Systems) were tested for inhibition spectrofluorometrically with C*sin*CPI-2 cystatin. Briefly, CTSK (266,91 nM) or CTSB (318,84 nM) was incubated in activity buffer (0.1 M sodium acetate buffer, 5 mM DTT, pH 5.5) in a final volume of 1 ml for 5 min at 37 °C. The fluorogenic substrate Z-Phe-Arg-AMC was added and the cysteine peptidase activity was measured in a continuous assay in a Shimadzu RF-5301PC spectrofluorometer at λex = 380 nm and λem = 460 nm. The active enzyme concentration was determined by titration with E-64 [30]. The inhibitory potential of C*sin*CPI-2 was determined through Cts residual enzymatic activity in a continuous assay after the addition of the inhibitor. The inhibition constants (K_i) were determined by fitting the steady-state kinetics velocities to the Morison equation for tight-binding inhibitors [32]. Briefly, by plotting $v_i/v_o = [I]/K_{i,app}$ (v_o represents velocity in the absence of an inhibitor and v_i represents velocity in the presence of an inhibitor) using the GraFit program (Erithacus Sofware, Horley, SRY, UK), $K_{i,app}$ values were obtained. Ki values were then calculated from the $K_{i,app}$ values using the equation $K_i = K_{i,app}/(1 + [S_0]/K_m)$, where the following K_m values were used to correct for the substrate competition: 17.84 μM – CTSK [33] and 23 μM – CTSB [34].

2.3. Anti-inflammatory activity of CsinCPI-2

The anti-inflammatory activity of *Csin*CPI-2 was evaluated in vitro through the analysis of its inhibitory effect on the gene expression of pro-inflammatory cathepsins K and B, and pro-inflammatory cytokines, TNF-α and interleukin-1 beta (IL-1β) in the mouse macrophage cell line RAW 264.7. In addition, the inhibitory effect of CsinCPI-2 on the activity of TNF-α in the bloodstream was also investigated in rats, in vivo.

2.3.1. In vitro study: Experimental design

2.3.1.1. Cell culture. The mouse macrophage cell line RAW 264.7 was cultured in DMEM (Dulbecco's Modified Eagle Medium, Thermo Fisher Scientific) supplemented with 10% fetal bovine serum, 100 U/ml of penicillin, 100 ug/ml of streptomycin under 5% CO_2 in a 95% humidified atmosphere at 37 °C until confluence.

2.3.1.2. Cell viability assay. Cell viability was measured through two different assays, Alamar Blue (Thermo Fisher Scientific) and Mitochondrial Dehydrogenase Enzymatic assay (MTT, Sigma-Aldrich, St. Luis, MO, USA) according to the manufacturer's instructions. A total of $5x10^4$ cells/ml were plated in 96-well plates, and the cells were exposed to different concentrations of *CsinCPI-2* (1.83 μM, 3.73 μM, 7.47 μM, 11.20 μM, and 16.60 μM) or α-MEM medium serum-free (negative control group) for 24 h. The Alamar Blue assay incorporates a fluorimetric redox indicator, and the fluorescence signal correlates with metabolic activity and the viability of the cells. The oxidation-reduction action was detected using a VERSAmax (Molecular Devices LLC, San Jose, CA, USA) microplate reader and was analyzed using its associated software, SoftMax®PRO 5 (Molecular Devices LLC). The MTT assay is based on the ability of mitochondrial dehydrogenase enzyme in converting the yellow water-soluble tetrazolium 3-(4,5-dimethyl-thiazolyl)-2,5-diphenyl-tetrazolium bromide into violet formazan compounds, whose absorbance is proportional to the number of living cells. The optical density (OD = 570 nm) was measured using a VERSAmax (Molecular Devices LLC) automated microplate reader.

2.3.1.3. Selection of the pro-inflammatory stimulus. RAW 264.7 cells were cultured on 6-well plates ($2x10^5$ cells/ml) and were stimulated with either LPS of *E. coli* (1 μg/ml- *E. coli* O111: B4, Sigma-Aldrich) or heat-inactivated bacteria *P. gingivalis* ATCC 3277 (10^7 UFC/ml and 10^8 UFC/ml) for 6, 12, and 24 h. Gene expression of cathepsins K, B, and TNF-α were measured by RT-qPCR.

2.3.1.4. Quantitative Real-Time PCR (RT-qPCR). RNA was isolated using an RNeasy kit (Qiagen) according to the instructions provided by the supplier. The cDNA was synthesized from 1 μg of total RNA using a High Capacity cDNA Reverse Transcription Kit (Applied Biosystems, Life Technologies, Grand Island, NY, USA). The gene expression was analyzed by qPCR in StepOne equipment (Applied Biosystems) using TaqMan chemistry and pre-designed primers and probe sets (Gene Expression Assays, Applied Biosystems). Primer/probe references were as follows: CTSK (Mm00484039_m1), CTSB (Mm01310506_m1), TNF-α (Mm00443259_g1), IL-1β (Mm01336189_m1), and the control GAPDH (Glyceraldehyde 3-phosphate dehydrogenase) (Mm99999915_g1) (Applied Biosystems). Duplicates were prepared for each reaction, and the experiment was repeated three times independently (n = 6/group). The determination of the relative levels of gene expression was performed using the cycle threshold method and normalized to the reference gene GAPDH. From this experiment, the best inflammatory stimulus was selected.

2.3.1.5. Inhibitory effect of Csin-CPI2 on pro-inflammatory cathepsins and cytokines. The RAW 264.7 cells were grown on 6-well plates (2×10^5 cells/ml). After confluence, the cells were stimulated with heat-inactivated bacteria *P. gingivalis* ATCC 3277 (10^7 UFC/ml) and treated with 3 different concentrations of *Csin*CPI-2: 3.73 μM, 7.47 μM, and 11.20 μM. The cells were collected at 12 and 24 h to measure the expression of cathepsins K and B and the cytokines TNF-α and IL-1ß. The samples were analyzed using RT-qPCR, as previously described.

2.3.2. In vivo study

2.3.2.1. Experimental design. The study was performed at the toxicology laboratory of the Natural Active Principles and Toxicology Department under the supervision of the Institutional Animal Care and Use Committee (CEUA #43/2015) of the School of Pharmaceutical Sciences (Sao Paulo State University - Unesp). Forty male Wistar rats weighing between 240 and 280 g were used. Femoral vein and artery catheters were surgically implanted. The experiment was divided into two stages. In the first stage, the animals (n = 5 per group) received single doses of *Csin*CPI-2 (0.82 mg/kg) via either IV or IP injection. In the second stage, they received *Csin*CPI-2 single doses of 0.4 mg/kg, 1.6 mg/kg, and 3.2 mg/kg via IP. Fifteen min after *Csin*CPI-2 administration, an IV dose of LPS (100 μg/kg) was administered in PBS followed by approximately 200 to 250 μl of blank saline. After, blood samples were collected at two time points (45 and 60 min) through a femoral arterial catheter into tubes with 25 μl of sodium heparin 5000 IU/ml (Hepamaz-S, Blau, Cotia, Brazil). The total blood withdrawn per animal was less than 1% of the animal body weight.

2.3.2.2. Bacterial preparation. The dose of LPS (*E. coli* O111: B4, #Lote# 091M4031, Aldrich-Sigma) was prepared in phosphate buffered saline solution (PBS, pH 7.2 to 7.4) at a concentration of 2 mg/ml. The dose volume used was 100 μg/kg administered via an IV. All doses of LPS were freshly prepared on the day of the study.

2.3.2.3. Determination of plasma TNF-α concentration. The blood samples were centrifuged at 500 rpm for 15 min. The plasma samples were collected and frozen at −20 °C until analysis. The plasma TNF-α levels were determined by a commercial ELISA kit (KRC3012, Thermo Fisher Scientific) and were carried out according to the manufacturer's instructions.

2.4. Pro-osteogenic effect of CsinCPI-2

2.4.1. Cell culture

hPDC was obtained following a protocol approved by the local research ethics committee (90278518.6.0000.5416). Cells were obtained from the third molars of 3 donor patients (18–25 years old) which were indicated for the extraction due to orthodontic reasons. Human pulp dental cells (hDPCs) were cultured in α-MEM medium (Sigma-Aldrich), supplemented with 10% fetal bovine serum, 100 U/ml of penicillin, 100 μg/ml of streptomycin, under 5% CO_2 in 95% humidified atmosphere at 37 °C until confluence. Cultured DPSCs in passage numbers from two to six were used for all the experiments with similar results.

2.4.2. Cell viability assay

Cell viability in hPDC was determined by the Alamar Blue and MTT assays. A total of $2x10^5$ cells/ml were plated in 96-well plates, and the cells were exposed to different concentrations (1.83 μM, 3.73 μM, 7.47 μM, 11.20 μM, and 16.60 μM) of *Csin*CPI-2 or α-MEM medium serum-free (negative control group) for 24 h. Dimethyl sulfoxide (DMSO) at a concentration of 20% was used as a positive control. The same methodology was used as described before.

2.4.3. Alkaline phosphatase (ALP) activity

A total of 7×10^4 cells/ml was plated in 96-well culture plates and exposed to *Csin*CPI-2 (1.83, 3.73, 7.47 e 16.60 μM) for 1, 3, 7, and 14 days. The ALP activity was evaluated using a commercial kit (Labtest; Lagoa Santa, MG, Brazil) and the absorbance was measured at 590 nm in a spectrophotometer. Three independent experiments were performed for each group, which were repeated six times. Data were expressed as the ALP activity normalized with the number of viable cells detected in the MTT assay in the respective culture period [35].

2.4.4. Alizarin red staining (ARS)

The hDPCs were plated (1×10^4 cells/ml) in 24-well culture plates with α-MEM osteogenic supplemented with 50 μg/ml of L-ascorbic acid (Sigma-Aldrich) and 10 mM β-glycerophosphate (Sigma-Aldrich). The hDPCs were exposed to *Csin*CPI-2 (3.73 μM) for 14 days. After that, the cells were stained with 2% Alizarin red S (pH 4.1). The mineralization

was quantified by dissolving the nodules with 500μl of 10% cetylpyridinium chloride solution (Sigma-Aldrich) and evaluating the optical density of the solution in a spectrophotometer at 562 nm. Three independent experiments were performed in triplicate for each experimental group.

2.4.5. RT-qPCR

hDPCs (2×10^5 cells/ml) were plated in 12-well plates. After 24 h of exposure to *Csin*CPI-2 (3.73 μM) diluted in serum-free medium, the RNA was extracted from the cells using Trizol (Invitrogen, Carlsbad, CA, USA) according to the instructions provided by the supplier. The gene expression was analyzed using qPCR, as described previously (2.3.1.4). Primer/probe references were as follows: bone morphogenetic protein-2, BMP-2 (Hs00154192_m1); osteocalcin, OC (Hs01587814_g1); alkaline phosphatase, ALP (Hs01029144_m1); bone sialoprotein, BSP (Bt03212717_g1), Runt-related transcription factor 2, RUNX-2 (Hs01047973_m1); and GAPDH (Hs02758991_g1). Each reaction was prepared in triplicate, and the experiment was repeated three times independently. The levels of target gene expression for each sample group were calculated with the ΔΔCt method (fold expression = $2^{-(\Delta\Delta Ct - stdev)}$) compared to the control.

3. Statistical analyses

Statistical analyses were performed using GraphPad Prism version 5.0 software (GraphPad Software Inc., San Diego, CA). An ANOVA followed by Bonferroni post hoc comparisons tests were used for the in vitro experiments. ARS assay data were compared using a *t*-test. An ANOVA followed by Tukey's post hoc tests were performed to analyze the inhibitory effect of *Csin*-CPI2 with raw cells. In the in vivo experiment, Kruskal-Wallis followed by Dunn's post hoc test was used for the intra- and inter-group analysis in the univariate analysis. In all the procedures, a significance level of 5% was adopted for the decision on the validity of the hypothesis tested.

4. Results

4.1. Heterologous expression and purification of CsinCPI-2

*Csin*CPI-2 (orange1.1g034261m - Phytozome) encodes a peptide with 100 amino acid residues with a molecular weight of 11.18 kDa and a pI of 6.73. Fig. 1 presents the multiple alignments between the amino acid sequences of *Csin*CPI-2 and other phytocystatins that presented a higher identity, highlighting the inhibitory motifs of cystatin and the characteristic phytocystatins motif, LARFAVDEHN. *Csin*CPI-2 protein presents a maximum of 67% identity with cystatins from other plants (ramie - *Boehmeria nivea* (ALG38347.1) − 67%, Nalita Wood *Trema orientalis* (POO01509.1) − 65%, *Parasponia andersonii* (PON74094.1) − 64%, and cassava – *Manihot esculenta* (XP_021604509.1) − 62%).

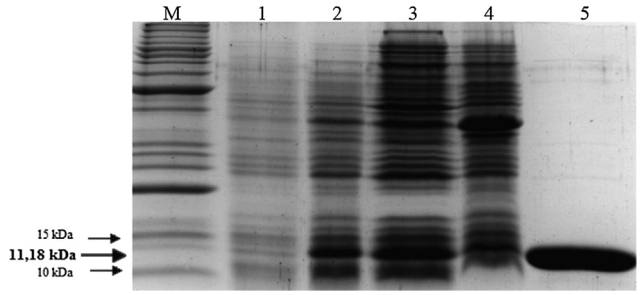

Fig. 2. The recombinant expression, solubility test, and purification of *Csin*CPI-2 protein. 15% SDS–PAGE stained with Coomassie blue showing in M: Benchmark molecular mass marker (Invitrogen); (1) non-induced culture; (2) crude extract of *E. coli* BL21(DE3) cells expressing *Csin*CPI-2 after 4 h of induction; (3) soluble fraction after the disruption of induced cells; (4) insoluble fraction after the disruption of induced cells; and (5) purified recombinant *Csin*CPI-2.

The phytocystatin C*sin*CPI-2 was recombinantly expressed in *E. coli* cells and was purified by immobilized metal affinity chromatography. The sodium dodecyl sulfate-polyacrylamide gel electrophoresis (SDS-PAGE) analysis revealed that cystatin was efficiently expressed in a soluble form with a molecular mass of approximately 11.00 kDa, as predicted from the amino acid sequence (Fig. 2). The yield of purified protein was approximately 10 mg/l of culture.

4.2. Inhibition of cysteine peptidases by CsinCPI-2

The ability of C*sin*CPI-2 cystatin to inhibit human CTSK and CTSB activity was assessed in a fluorometric assay. The residual hydrolytic activity of enzymes was measured after pre-incubation with the inhibitor added at increasing concentrations. The results indicate that the activity of CTSK was significantly inhibited by C*sin*CPI-2 with k_i of 5.15 nM, showing a strong interaction between the enzyme and inhibitor. In general, phytocystatins show good inhibitory activity against human cathepsins [23,25,26,36]. However, whereas C*sin*CPI-2 was able to inhibit CTSK, it showed weak inhibition of CTSB.

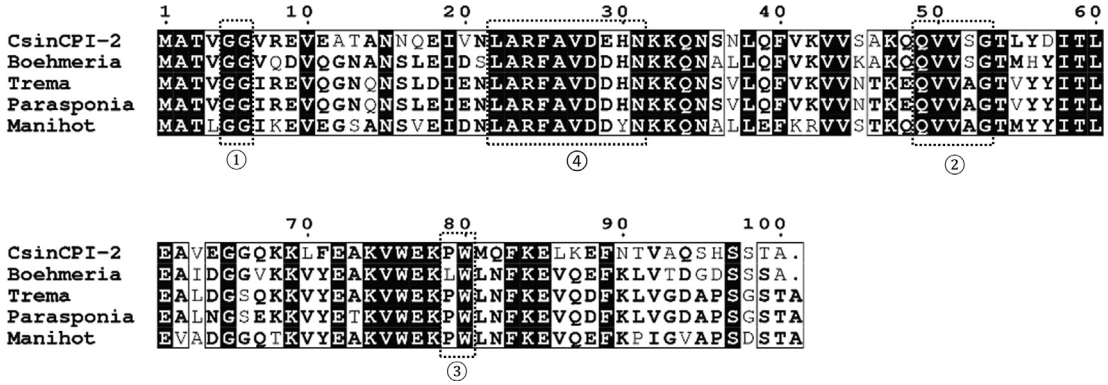

Fig. 1. The multiple alignment analysis of the amino acid sequences of CsinCPI-2 and phytocystatins that present a higher sequence identity with the protein. CsinCPI-2 protein presents a maximum identity with ramie – *Boehmeria nivea* (ALG38347.1) − 67%, Nalita Wood *Trema orientalis* (POO01509.1) − 65%, *Parasponia andersonii* (PON74094.1) − 64%, and cassava - *Manihot esculenta* (XP_021604509.1) − 62%. Conserved identical residues are marked in black boxes and white boxes to show conserved residues with more than 50% identity. The regions highlighted by dotted boxes indicate the papain-like inhibitory motifs: (1) GG, (2) PW, (3) QxVxG, and (4) the exclusive phytocystatins motif: [LVI] - [AGT] - [RKE] - [FY] - [AS] - [VI] -X- [EDQV] - [HYFQ] - N. The alignment was generated using the Multalin program with default parameters.

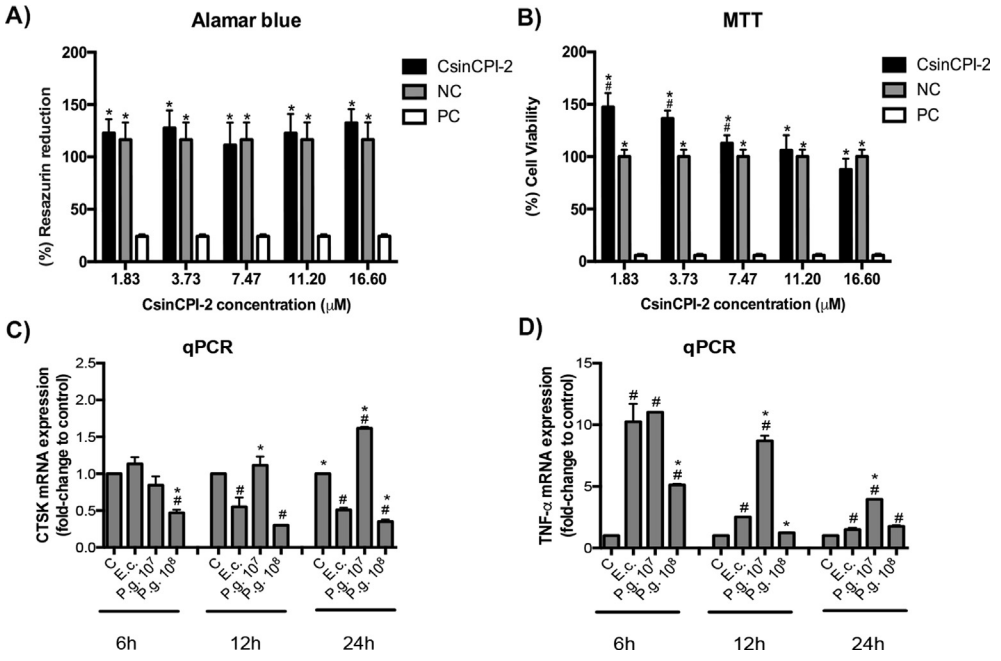

Fig. 3. Effect of *Csin*CPI-2 on cellular viability (A-B) and the selection of a pro-inflammatory stimulus (C-D). Raw 264.7 cells (5×10^4) were grown in 96-well plates, incubated for 24 h with different concentrations (1.83 μM, 3.73 μM, 7.47 μM, 11.20 μM, and 16.60 μM) of *Csin*CPI-2 or a-MEM medium serum-free (negative control group) and 20% dimethyl sulfoxide (DMSO) (positive control), which were evaluated by Alamar Blue (A) and MTT (B) assays. Cells were also stimulated with LPS of *E. coli* (1 μg/ml) with heat-inactivated bacteria *P. gingivalis* ATCC 3277 (10^7 UFC/ml and 10^8 UFC/ml) or a-MEM medium serum-free (negative control group), the pro-inflammatory stimulus was determined by the mRNA expression of CTSK (C) and TNF-α (D) genes in RAW 264.7 cells after 6, 12, and 24 h of treatment. PC, positive control. NC, negative control. C. Negative control. P.g. 10^7, *P. gingivalis* (10^7 UFC/ml). P.g. 10^8, *P. gingivalis* (10^8 UFC/ml). LPS, LPS of *E. coli.* In A and B: * represents a statistical difference ($p < 0.05$) from the PC; # represents a statistical difference ($p < 0.05$) from the NC. In C and D: * represents a statistical different ($p < 0.05$) from the LPS of *E. coli*; # represents a statistical difference ($p < 0.05$) from the control (n = 6).

4.3. In vitro anti-inflammatory activity of CsinCPI-2

4.3.1. Cell viability assay on RAW 264.7 cells

Alamar Blue and MTT (Mitochondrial Dehydrogenase Enzymatic) assays revealed that *Csin*CPI-2 had no cytotoxic effects for all the tested concentrations in Raw 264.7 cells, the viability was similar to the negative control ($P > 0.05$) (Fig. 3).

4.3.2. Selection of inflammatory stimulus

To select the inflammatory stimulus, mouse macrophage cell line Raw 264.7 cells were stimulated with bacterial LPS of *E. coli* (1ug/ml) or with heat-inactivated bacteria *P. gingivalis* ATCC 3277 (10^7 UFC/ml and 10^8 UFC/ml) and were measured using RT-qPCR after 6, 12, and 24 h. The heat-inactivated bacteria *P. gingivalis* (10^7 UFC/ml) presented a higher expression of CTSK than the LPS of *E. coli* and *P. gingivalis* (10^8 UFC/ml) after 12 and 24 h of the stimulus. TNF-α presented an increased expression at 6, 12, and 24 h time points with all the stimulus. Again, *P. gingivalis* 10^7 UFC/ml induced a significantly higher stimulus at 12 and 24 h (Fig. 3).

4.3.3. Effect of CsinCPI-2 activity on mRNA expression of cysteine peptidases and proinflammatory cytokines

Raw 264.7 cells were stimulated with *P. gingivalis* 10^7 UFC/ml and were treated with 3 different concentrations of *Csin*CPI-2 (3.73 μM, 7.47 μM, and 11.20 μM). After 12 and 24 h, the mRNA expressions of cysteine peptidases (CTSK and CTSB) and pro-inflammatory cytokines (TNF-α and IL-1β) were evaluated by PCR (RT-qPCR). The CTSK mRNA expression decreased in both periods for all concentrations of *Csin*CPI-2. After 12 h, CTSB showed no statistical difference in all the groups tested; however, at 24 h and in both concentrations (3.73 μM and 7.47 μM), a significant decrease in the mRNA expression ($P < 0.05$) was detected (Fig. 4). TNF-α and IL-1β mRNA expressions were increased in all the groups after 12 h of the stimulus. At the 24 h time point, TNF-α mRNA expression decreased in all the groups exposed to *Csin*CPI-2. The IL-1β mRNA expression also decreased in all the tested concentrations, but a statistical difference in relation to *P. gingivalis* 10^7 UFC/ml and the control group ($P < 0.05$) was only detected in the 7.47 μM concentration (Fig. 4).

4.4. In vivo anti-inflammatory activity of CsinCPI-2.

4.4.1. Effect of CsinCPI-2 on the TNF-α in the bloodstream of rats

First stage: The effect of *Csin*CPI-2 (0.82 mg/kg), administered via intravenous (IV) and intraperitoneal (IP) injection, on the activity of TNF-α in the bloodstream of rats was assessed using an ELISA Test at two time points (45 and 60 min) after a challenge with 100 μg/kg LPS. At the 45 min time point, the activity of TNF-α decreased, and after 60 min both routes of administration (IP and IV) showed a statistical difference compared to the LPS group (Fig. 5).

Second stage: The effect of *Csin*CPI-2 in different concentrations (0.4 mg/kg, 0.82 mg/kg, 1.6 mg/kg, and 3.2 mg/kg), administered via an IP injection, on the activity of TNF-α in the bloodstream of rats was measured using an ELISA Test at 2 time points (45 and 60 min) after a 100 μg/kg LPS challenge (IV). At 45 min, the activity of TNF-α decreased in all the concentrations tested administered via an IP injection; it reached a significant statistical difference at 60 min at a concentration of 0.82 mg/kg when compared to the LPS group. (Fig. 5)

4.5. Pro-osteogenic effect of CsinCPI-2

4.5.1. Cell viability assay on hDPCs

Alamar Blue and MTT viability assays revealed that *Csin*CPI-2 had no cytotoxic effects for all the tested concentrations in hDPCs. In the Alamar Blue assay, there was no significant difference in the cell viability at the tested concentrations when compared to the negative control ($P > 0.05$). In the MTT assay, the cell viability was higher for all the concentrations compared to the negative control ($P < 0.05$) (Fig. 6).

4.5.2. ALP activity

On the first day of hDPC exposure to *Csin*CPI-2, there were no cytotoxic effects in all the tested concentrations when compared to the control ($P > 0.05$). At the 3rd and 7th days, the hDPC viability exposed to *Csin*CPI-2 was similar ($P > 0.05$) or lower than the control

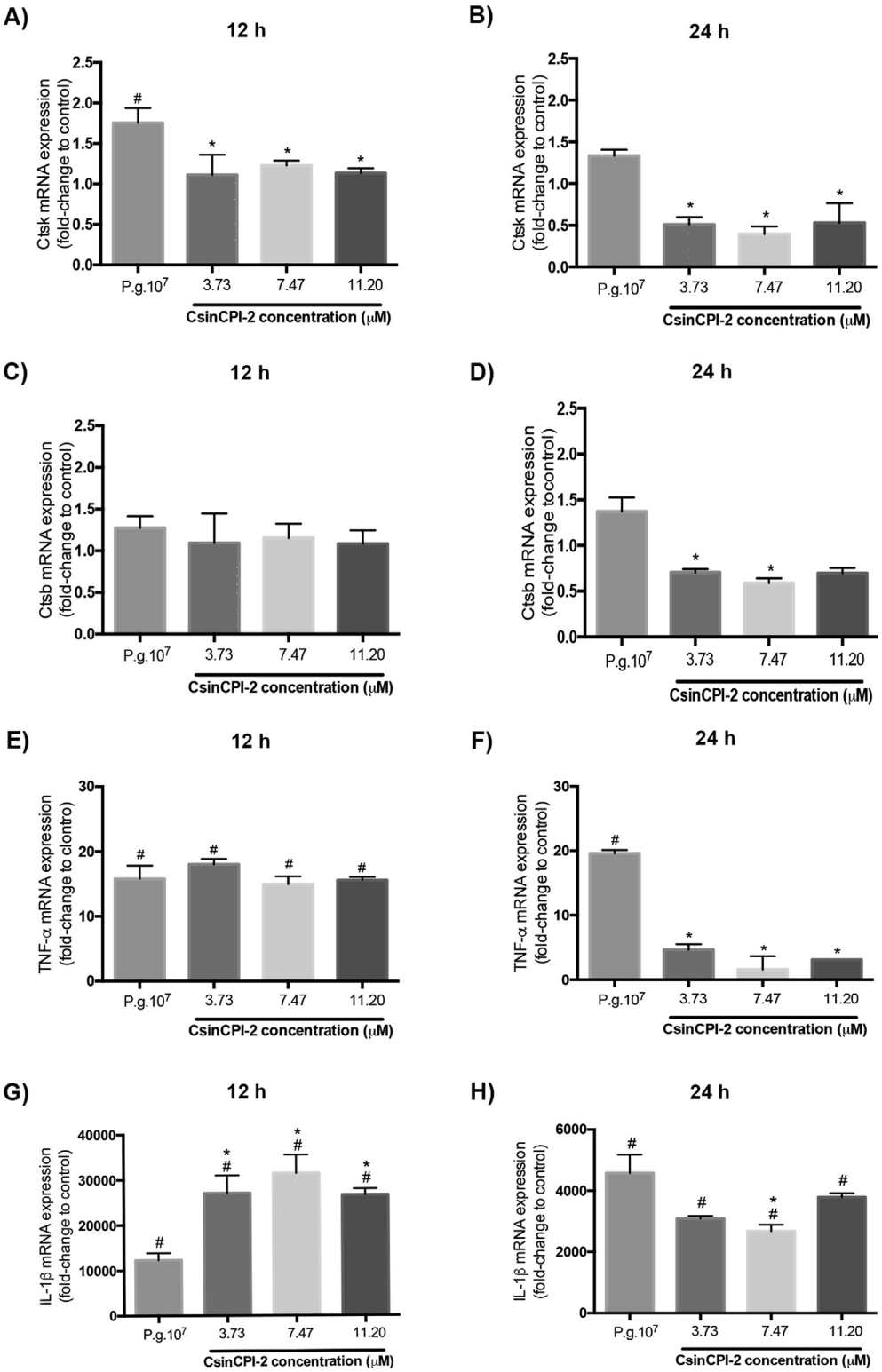

Fig. 4. Effect of *Csin*CPI-2 activity on cathepsin and cytokine gene expression. CTSK (A-B) and CTSB (C-D), TNF- α(E-F), and IL-1β (G-I) mRNA expression in Raw 264.7 cells (2×10^5 cell/well) after 12 and 24 h of *P. gingivalis* 10^7 UFC/ml stimulus, and treatment with different concentrations of *Csin*CPI-2. The phytocystatin inhibited the expression of CTSK gene after 12 and 24 h and CTSB gene after 24 h of treatment with *Csin*CPI-2. # represents a statistical difference ($p < 0.05$) from the control; * represents a statistical difference from the LPS of *E. coli.* (n = 6). Pg7, *P. gingivalis* (10^7 UFC/ml).

($P < 0.05$). At the 14th day, the hDPCs exposed to *Csin*CPI-2 at low concentrations (1.83 and 3.73 μM) had a higher cell viability than the control ($P < 0.05$). The ALP activity was inversely proportional to the concentration of *Csin*CPI-2, that is, at lower concentrations, there was a higher activity of ALP. The highest ALP activity ($P < 0.05$) was observed at the 7th and 14th day of treatment with *Csin*CPI-2 at the lowest concentrations (1.83 and 3.73 μM), as shown in Fig. 7A.

4.5.3. Alizarin red staining (ARS)

After 14 days of hDPC exposure, *Csin*CPI-2 (3.73 μM) had a

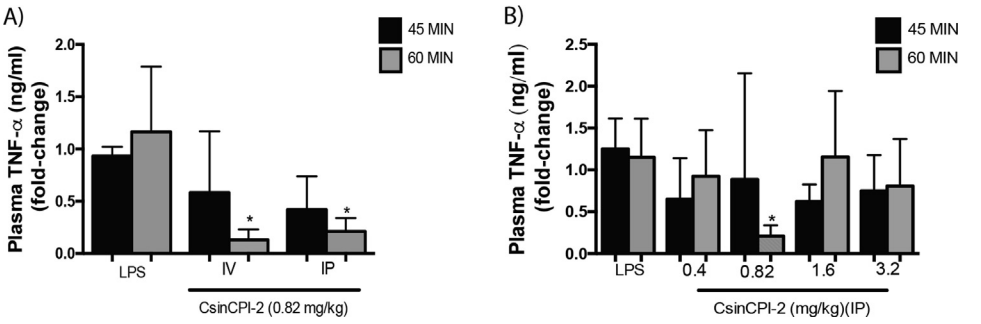

Fig. 5. In vivo anti-inflammatory effect of *Csin*CPI-2 in the plasma of rats. (A) Plasma concentration time profiles (45 and 60 min) of TNF-α after IV and IP (0.82 mg/kg) administration of *Csin*CPI-2 followed by 100 μg/kg LPS stimulation. (B) Plasma concentration time profiles (45 and 60 min) of TNF-α after IP (0.4 mg/kg, 0.82 mg/kg, 1.6 mg/kg, and 3.2 mg/k) administration of *Csin*CPI-2 followed by 100 μg/kg LPS stimulation. * represents a statistical difference from the LPS ($p < 0.05$) ($n = 5$).

significant stimulatory effect on the formation of mineralized nodules ($P < 0.05$) when compared to the control (Fig. 7B).

4.5.4. Quantitative real-time PCR

At day one and three, the hDPCs exposed to *Csin*CPI-2 (3.73 μM) overexpressed BMP-2 by 40 and 108 times, respectively, in relation to the control group ($P < 0.05$). At days 7 and 14, the hDPCs exposed to *Csin*CPI-2 had an increase in RUNX-2 mRNA expression by approximately 1.9- and 1.4-fold, respectively, compared to the control ($P < 0.05$). ALP mRNA expression had an increase of approximately 1.15-fold at 7 days ($P < 0.05$), OC increased at 3 days (approximately 1.36-fold increase), and at 7 days (approximately 1.21-fold increase) ($P < 0.05$), BSP mRNA expression was high (approximately 1.43-fold increase) in the first day of exposure to *Csin*CPI-2 ($P < 0.05$), as shown in Fig. 8.

5. Discussion

In the present study, it was reported for the first time that phytocystatin *Csin*CPI-2 has a potential anti-inflammatory effect, through the inhibition of inflammatory cysteine peptidases (CTSK and CTSB) and cytokines (TNF-α and IL-1β) in mouse macrophage cells in vitro.

It was demonstrated that the protein C*sin*CPI-2 has different inhibitory effects against human CTSB and CTSK, which correlates with their ability to inhibit cellular cysteine peptidase activity. C*sin*CPI-2 inhibits the enzymatic activity of human CTSK in vitro, presenting a $K_i = 5.15$ nM. A weak in vitro inhibition of CTSB by C*sin*CPI-2 at pH 5.5 was observed. CTSB possesses endopeptidase and exopeptidase activity, which is attributed to the presence of the occluding loop [5]. CTSB presents exopeptidase activity with an optimal pH of around 5 and endopeptidase at a neutral pH [37–40]. The weak inhibition of CTSB by *Csin*CPI-2 in vitro may be partially explained by the differential activity of CTSB in different pH values.

The distinct K_i values reported here, particularly for CTSK, can be correlated with the anti-inflammatory activity of *Csin*CPI-2 evaluated in vitro through the analysis of the inhibitory effect on the gene expression of the pro-inflammatory CTSK in the mouse macrophage cell line RAW 264.7, treated with different concentrations of *Csin*CPI-2. The effect of *Csin*CPI-2 activity on the mRNA expression of cysteine peptidases was evaluated using RT-qPCR. After 12 h, the mRNA expression of CTSK decreased for all the concentrations of *Csin*CPI-2. After 12 h, CTSB showed no statistical difference in all the tested groups; however, at 24 h, a significant decrease in mRNA expression was detected. In addition, TNF-α activity in the bloodstream was also inhibited, in rats, in vivo. These results corroborate with in vitro assays of cathepsin inhibition in this work and previous studies showing inhibitory effects of phytocystatins derived from sugarcane on cathepsins B, K, V, and L, as well as on the invasive ability of breast cancer cells [21,23,26].

In an inflammatory environment, cytokines stimulate resident and infiltrated cells and enhance the receptor activator of NF-kB ligand (RANKL), leading to osteoclast formation and bone loss [41]. CTSK is highly expressed in osteoclasts, and it plays a key role in matrix degradation [4,41]. Therefore, it has been considered as an important target enzyme for cysteine peptidase inhibitors involved in bone resorption [4]. Hence, CsinCPI-2 presents a promising effect of inhibiting osteoclastogenesis and bone loss.

Supporting our results, Cys C has also been shown to inhibit CTSK mRNA in mouse bone marrow macrophage cultures [42]. This effect of CTSK by Cys C has also resulted in the inhibition of the osteoclastogenesis [43]. A deficiency of CTSK in mice by gene deletion showed a significant reduction in inflammation and bone erosion in rheumatoid arthritis (RA) joint capsules and in experimental periodontitis mouse models [8]. In addition, CTSK deficient mice presented a decrease in the infiltration of the immune cells, a reduction in the number of osteoclasts and macrophages, and the downregulation of the expression of TLR-4, 5, and 9 and their downstream cytokines in gingival epithelial lesions and synovial RA lesions [8].

In the present study, besides cathepsins, *Csin*CPI-2 also inhibited the

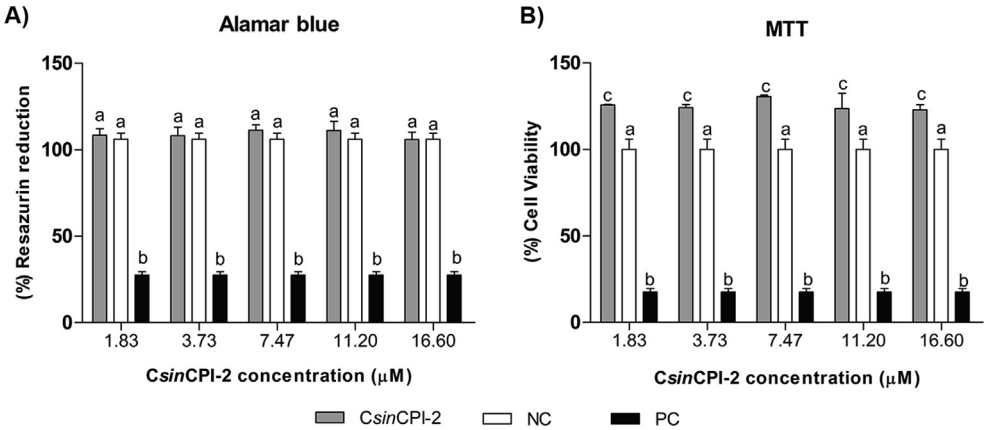

Fig. 6. Human dental pulp cell (hDPC) viability after exposure to *Csin*CPI-2 for 24 h. (A) Alamar Blue and (B) MTT assays in hDPCs exposed to different concentrations of *Csin*CPI-2 or a serum-free MEM medium (negative control group) and 20% dimethyl sulfoxide – DMSO (positive control) for 24 h.

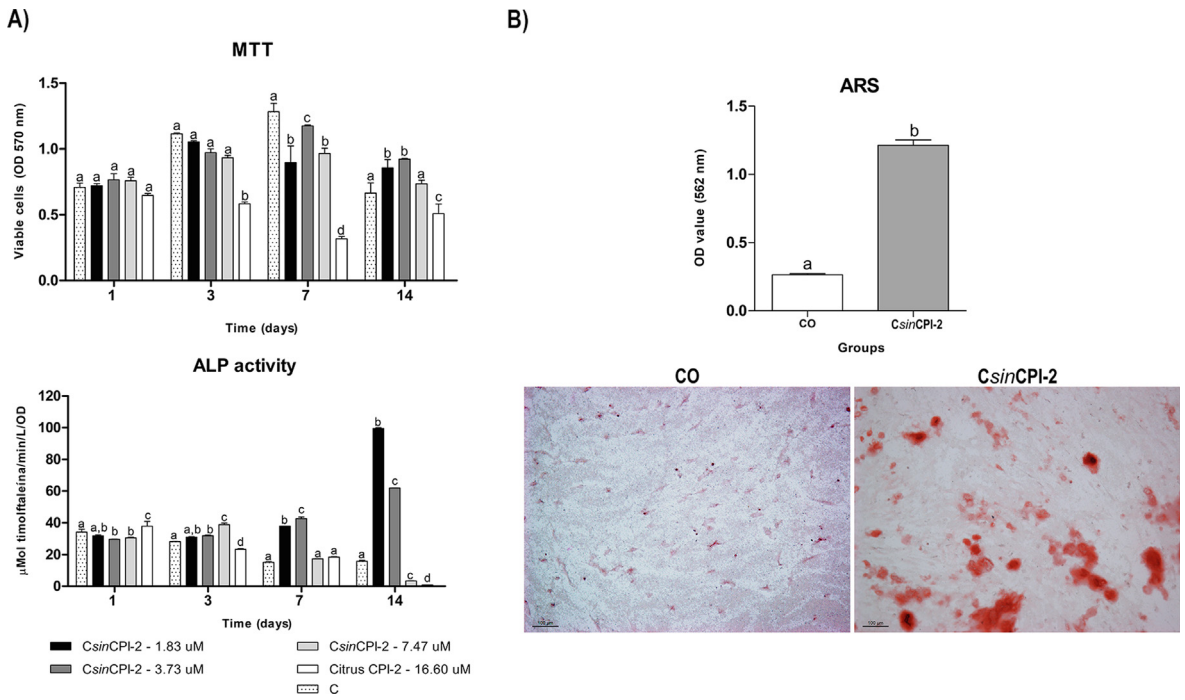

Fig. 7. The pro-osteogenic effect of *Csin*CPI-2 in human dental pulp cells (hDPCs) evaluated by alkaline phosphatase (ALP) activity and alizarin red staining (ARS). (A) hDPC viability by MTT assay and ALP activity after exposure to *Csin*CPI-2 in different concentrations and to the culture medium (control) for 1, 3, 7, and 14 days. (B) ARS assay showing the comparison of mineralized nodule production and figures of the *Csin*CPI-2 (3.73 µM) group showing the mineralized nodule deposition (red) and the osteogenic control group after 14 days of *Csin*CPI-2 exposure. Bars with different letters represent a significant difference between the groups: CO, osteogenic control. (For interpretation of the references to colour in this figure legend, the reader is referred to the web version of this article.)

expression of pro-inflammatory cytokines TNF-α and IL-1β in vitro and in vivo. Other studies have shown that when the activity of the cysteine peptidases is inhibited, the expression of the pro-inflammatory cytokines is also downregulated [7–9]. Ha found that CTSB is involved in the transportation of TNF-α into the plasma membrane, inhibition of the activity to CTSB affects this cytokine inhibiting its expression [11]. A previous study showed that TNF-α and IL-1β stimulates the production of CTSB on synovial fibroblast cells of patients with RA and osteoarthritis [44,45]. In the in vivo study, *Csin*CPI-2 showed an inhibitory effect on the activity of TNF-α in the bloodstream in rats after an LPS challenge. Other studies found similar results, demonstrating that blocking the activity of cathepsins results in the downregulation of the expression of pro-inflammatory cytokines [8,9]. Chen et al. used gene therapy to silence CTSK in a mouse model of periodontitis, and their results showed an inhibitory effect on the cytokines involved in inflammation, like TNF-α [7].

The model of the induction of TNF-α production, and release in the bloodstream after LPS of *E. coli* stimulus used in the in vivo study was established in the literature [46]. However, the synthesis and release of TNF-α depends on each animal and can vary during the response to an LPS challenge. This resulted in a high standard deviation among the animals of the LPS-stimulated group, as can be seen in Fig. 5.

The data showed a significant increase of TNF-α in the blood plasma after an LPS IV challenge at 45 min, and the maximum peak at 60 min in the LPS-stimulated group, with values between 7 and 8 ng/ml. Similar results were observed in the study by Wang et al. [46], where TNF-α production started to increase at 30 min and reached its maximum production at 90 min, suffering a rapid fall 3 to 4 h after the LPS challenge. The TNF-α plasma values were between 8 and 10 ng/ml. In the present study, the samples were analyzed by an ELISA test at 45 min and 60 min as these time points were when the concentration of TNF-α was the highest. Although four different concentrations of *Csin*CPI-2 were tested using IP administration, the concentration of 0.82 mg/kg showed the best inhibitory effect of the phytocystatin. The findings suggest that lower concentrations are not enough to inhibit TNF-α and higher concentrations may produce additional effects interfering in the inhibitory effect of cathepsins. A higher concentration may stimulate the resorption of receptors or may stimulate another pathway leading to an effect that is opposed to the primary effect of the compound. Therefore, pharmacokinetic and pharmacodynamic studies of phytocystatin *Csin*CPI-2 are indicated, to ascertain the pathways and molecules involved in the action of the phytocystatins in a defined period of time. With these further studies, it will be possible to determine the concentration and route of administration suitable to carry out an effective treatment with the adequate use of *Csin*CPI-2.

In the present study, the pro-osteogenic effect of *Csin*CPI-2 was also evaluated in vitro using hDPCs. The lower concentrations of CsinCPI-2 (1.83 µM and 3.73 µM) showed no cytotoxicity and induced high ALP activity. For this reason, we chose an intermediate concentration (3.73 µM) of CsinCPI-2 for the qPCR and ARS assays in hDPCs.

BMP-2, a member of the transforming growth factor beta (TGF-β) superfamily, plays a decisive role during bone formation, regeneration, and the repair process [47,48]. *Csin*CPI-2 stimulated an increase in the mRNA expression of the osteogenic marker BMP-2 at 1 and 3 days of exposure. According to the literature, the inhibitors of cysteine protease can stimulate BMP-2 expression [22], and suppress the degradation of growth factors, such as BMP-2, in the organic matrix, consequently increasing bone formation [49]

The RUNX-2 osteogenic marker coordinates multiple signaling pathways related to the differentiation of osteoblasts [50]. There was an increase in RUNX-2 mRNA expression at 7 and 14 days after the exposure of hDPCs to *Csin*CPI-2 when compared to the control group. Teti et al. showed that hDPCs in contact with carboxymethylcellulose hydrogel and hydroxyapatite had increased RUNX-2 mRNA expression at 7, 14, and 21 days, which corroborates with the RUNX-2 expression periods in our study.

OC, which regulates the mineral phase of bone, is a marker of the late stages of osteogenic differentiation [24,51]. BSP is mainly secreted by osteoblasts, and its expression is a crucial symbol in matrix deposition and mineralization [52,53]. Increased BSP expression suggests

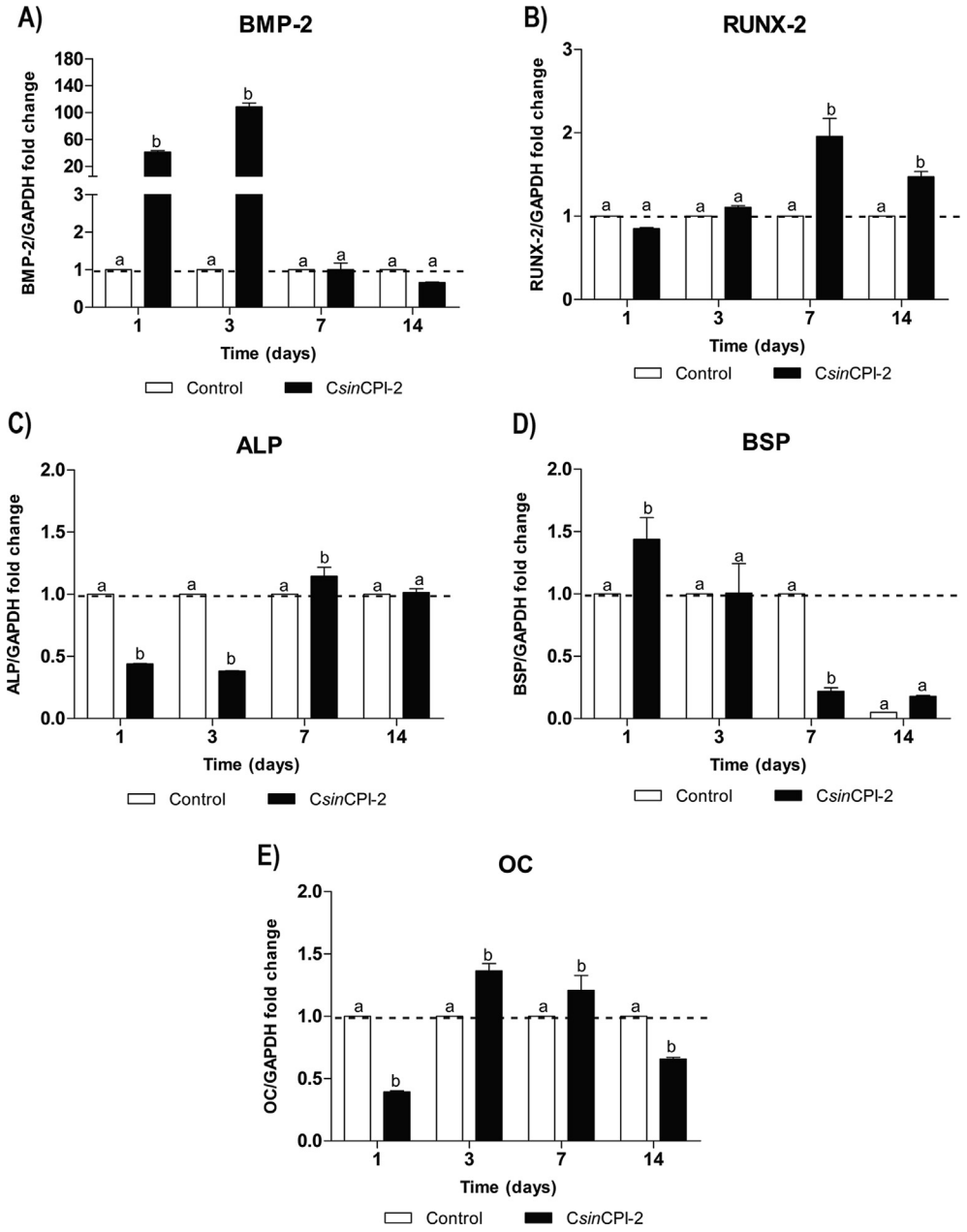

Fig. 8. The pro-osteogenic effect of *Csin*CPI-2 in human dental pulp cells (hDPCs) evaluated by qPCR. mRNA expression levels of target genes in hDPCs exposed to *Csin*CPI-2 (3.73 μM) for 1, 3, 7, and 14 days. Bars with different letters represent a statistically significant difference between the groups in each experimental period. BMP-2, bone morphogenetic protein 2; OC, osteocalcin; ALP, alkaline phosphatase; BSP, bone sialoprotein; RUNX 2, runt-related transcription factor 2 genes; C, cells exposed to serum free α-MEM medium.

the differentiation of several cells into osteoblasts [54]. ALP has been implicated in several key roles in skeletal mineralization. In the present study, there was an increase in mRNA expression of the osteogenic markers OC, BSP, and ALP in hDPCs treated with *Csin*CPI-2.

ALP is one of the major enzymes expressed during the early maturation of osteoblasts and plays an important role in mineral deposition [55]. The increase in ALP activity indicates an increase in the expression of osteoblastic phenotypes [56]. The alizarin red staining assay allows the quantification of calcium deposits in cell cultures [57]; *Csin*CPI-2 stimulated ALP activity and the deposition of mineralized nodules. Therefore, considering these results and the increased expression of osteogenic markers, *Csin*CPI-2 induced hDPC differentiation in osteogenic phenotypes. These results are in line with a study that treated the cells of the bone marrow and calvaria bone marrow with cystatin C (CysC) which is a natural inhibitor of cysteine protease that suppresses the differentiation and function of osteoclast reabsorption. The authors showed that Cys C increased ALP activity, mineralized nodule formation, and increased BMP-2, RUNX-2, and OC mRNA expression [18].

6. Conclusion

This study demonstrated that *Csin*CPI-2 has a potential anti-inflammatory effect and at the same time, a pro-osteogenic effect. This may lead to new therapies for the control of inflammatory diseases, such as periodontal disease and apical periodontitis.

Declaration of Competing Interest

The authors declare no conflict of interest.

Acknowledgements

We thank Dr. Rosângela Gonçalves Peccinini [Department of Natural Active Principles and Toxicology, School of Pharmaceutical Sciences, São Paulo State University, Araraquara, Brazil], for helpful collaboration while working in the Toxicology Laboratory.

Funding

This study was supported by the Brazilian National Council for Scientific and Technological Development [CNPq 486335/2013-5]; Coordination of the Improvement of Higher Education Personnel – (CAPES 2016/1604159] and [CAPES/PROEX]; by São Paulo Research Foundation (FAPESP 2017/05784-0]; and Organization of American States and Coimbra Group of Brazilian Universities [OEA-GCUB-2014].

References

[1] H.F. Galley, N.R. Webster, The immuno-inflammatory cascade, Br. J. Anaesth. 77 (1996) 11–16, https://doi.org/10.1093/bja/77.1.11.
[2] T.M. Wright, Cytokines in acute and chronic inflammation, Front. Biosci. 2 (1997) A171, https://doi.org/10.2741/A171.
[3] S.M. Jung, K.W. Kim, C. Yang, S. Park, J.H. Ju, Cytokine-mediated bone destruction in rheumatoid arthritis, J. Immunol. Res. 2014 (2014) 1–15, https://doi.org/10.1155/2014/263625.
[4] M. Brage, M. Abrahamson, V. Lindström, A. Grubb, U.H. Lerner, Different cysteine proteinases involved in bone resorption and osteoclast formation, Calcif. Tissue Int. 76 (2005) 439–447, https://doi.org/10.1007/s00223-004-0043-y.
[5] V. Turk, V. Stoka, O. Vasiljeva, M. Renko, T. Sun, B. Turk, D. Turk, Cysteine cathepsins: From structure, function and regulation to new frontiers, Biochim. Biophys. Acta – Proteins Proteomics 2012 (1824) 68–88, https://doi.org/10.1016/j.bbapap.2011.10.002.
[6] T. Laitala-Leinonen, R. Rinne, P. Saukko, H.K. Väänänen, A. Rinne, Cystatin B as an intracellular modulator of bone resorption, Matrix Biol. 25 (2006) 149–157, https://doi.org/10.1016/j.matbio.2005.10.005.
[7] W. Chen, B. Gao, L. Hao, G. Zhu, J. Jules, M.J. MacDougall, J. Wang, X. Han, X. Zhou, Y.P. Li, The silencing of cathepsin K used in gene therapy for periodontal disease reveals the role of cathepsin K in chronic infection and inflammation, J. Periodontal Res. 51 (2016) 647–660, https://doi.org/10.1111/jre.12345.
[8] L. Hao, G. Zhu, Y. Lu, M. Wang, J. Jules, X. Zhou, W. Chen, Deficiency of cathepsin K prevents inflammation and bone erosion in rheumatoid arthritis and periodontitis and reveals its shared osteoimmune role, FEBS Lett. 589 (2015) 1331–1339, https://doi.org/10.1016/j.febslet.2015.04.008.
[9] Peter Schotte, Reinout Schauvliege, Sophie Janssens, Rudi Beyaert, The cathepsin B inhibitor z-FA.fmk inhibits cytokine production in macrophages stimulated by lipopolysaccharide, J. Biol. Chem. 276 (24) (2001) 21153–21157, https://doi.org/10.1074/jbc.M102239200.
[10] D.P. Dickinson, Cysteine peptidases of mammals: their biological roles and potential effects in the oral cavity and other tissues in health and disease, Crit. Rev. Oral Biol. Med. 13 (2002) 238–275, https://doi.org/10.1177/154411130201300304.
[11] S.-D. Ha, A. Martins, K. Khazaie, J. Han, B.M.C. Chan, S.O. Kim, Cathepsin B is involved in the trafficking of TNF-alpha-containing vesicles to the plasma membrane in macrophages, J. Immunol. 181 (2008) 690–697, https://doi.org/10.4049/jimmunol.181.1.690.
[12] J. Hannaford, H. Guo, X. Chen, Involvement of cathepsins B and L in inflammation and cholesterol trafficking protein NPC2 secretion in macrophages, Obesity. 21 (2013) 1586–1595, https://doi.org/10.1002/oby.20136.
[13] N.Y.C. Yu, A. Fathi, C.M. Murphy, K. Mikulec, L. Peacock, L.C. Cantrill, F. Dehghani, D.G. Little, A. Schindeler, Local co-delivery of rhBMP-2 and cathepsin K inhibitor L006235 in poly(d, l-lactide-co-glycolide) nanospheres, J. Biomed. Mater. Res. - Part B Appl. Biomater. 105 (2017) 136–144, https://doi.org/10.1002/jbm.b.33481.
[14] L.T. Duong, A.T. Leung, B. Langdahl, Cathepsin K inhibition: a new mechanism for the treatment of osteoporosis, Calcif. Tissue Int. 98 (2016) 381–397, https://doi.org/10.1007/s00223-015-0051-0.
[15] J. Ochieng, G. Chaudhuri, Cystatin superfamily, J. Health Care Poor Underserved. 21 (2010) 51–70, https://doi.org/10.1353/hpu.0.0257.
[16] Y.M. Henskens, E.C. Veerman, M.S. Mantel, U. van der Velden, A.V. Nieuw Amerongen, Cystatins S and C in human whole saliva and in glandular salivas in periodontal health and disease, J. Dent. Res. 73 (1994) 1606–1614, https://doi.org/10.1177/00220345940730100501.
[17] E.M. Reis, R. Margis, Sugarcane phytocystatins: Identification, classification and expression pattern analysis, Genet. Mol. Biol. 24 (2001) 291–296, https://doi.org/10.1590/S1415-47572001000100038.
[18] A. Danjo, T. Yamaza, M.A. Kido, D. Shimohira, T. Tsukuba, T. Kagiya, Y. Yamashita, K. Nishijima, S. Masuko, M. Goto, T. Tanaka, Cystatin C stimulates the differentiation of mouse osteoblastic cells and bone formation, Biochem. Biophys. Res. Commun. 360 (2007) 199–204, https://doi.org/10.1016/j.bbrc.2007.06.028.
[19] H. Kondo, K. Abe, Y. Emori, S. Arai, Gene organization of oryzacystatin-II, a new cystatin superfamily member of plant origin, is closely related to that of oryzacystatin-I but different from those of animal cystatins, FEBS Lett. 278 (1991) 87–90, https://doi.org/10.1016/0014-5793(91)80090-P.
[20] R. Margis, E.M. Reis, V. Villeret, Structural and phylogenetic relationships among plant and animal cystatins, Arch. Biochem. Biophys. 359 (1998) 24–30, https://doi.org/10.1006/ABBI.1998.0875.
[21] A. Soares-Costa, L.M. Beltramini, O.H. Thiemann, F. Henrique-Silva, A sugarcane cystatin: Recombinant expression, purification, and antifungal activity, Biochem. Biophys. Res. Commun. 296 (2002) 1194–1199, https://doi.org/10.1016/S0006-291X(02)02046-6.
[22] A. Gianotti, W.M. Rios, A. Soares-Costa, V. Nogaroto, A.K. Carmona, M.L.V. Oliva, S.S. Andrade, F. Henrique-Silva, Recombinant expression, purification, and functional analysis of two novel cystatins from sugarcane (Saccharum officinarum), Protein Expr. Purif. 47 (2006) 483–489, https://doi.org/10.1016/j.pep.2005.10.026.
[23] A. Gianotti, C.A. Sommer, A.K. Carmona, F. Henrique-Silva, Inhibitory effect of the sugarcane cystatin CaneCPI-4 on cathepsins B and L and human breast cancer cell invasion, Biol. Chem. 389 (2008) 447–453, https://doi.org/10.1515/BC.2008.035.
[24] J.P. Oliveira, H.F. Magliarelli, F.V. Pereira, A. Gianotti, A. Soares-Costa, F. Henrique-Silva, A. Wakamatsu, I.C. Soares, S. Nonogaki, L.R. Travassos, A.K. Carmona, T. Paschoalin, Sugarcane cystatin caneCPI-4 inhibits melanoma growth by angiogenesis disruption, J. Cancer Sci. Ther. 3 (2011) 161–167, https://doi.org/10.4172/1948-5956.1000081.
[25] A.C.C. Santiago, Z.N.N. Khan, M.C.C. Miguel, C.C.C. Gironda, A. Soares-Costa, V.T.T. Pelá, A.L.L. Leite, J.M.M. Edwardson, M.A.R.A.R. Buzalaf, F. Henrique-Silva, A new sugarcane cystatin strongly binds to dental enamel and reduces erosion, J. Dent. Res. 96 (2017) 1051–1057, https://doi.org/10.1177/0022034517712981.
[26] M.L. Vilela Oliva, A.K. Carmona, S.S. Andrade, S.S. Cotrin, A. Soares-Costa, F. Henrique-Silva, Inhibitory selectivity of canecystatin: A recombinant cysteine peptidase inhibitor from sugarcane, Biochem. Biophys. Res. Commun. 320 (2004) 1082–1086, https://doi.org/10.1016/j.bbrc.2004.06.053.
[27] D.M. Goodstein, S. Shu, R. Howson, R. Neupane, R.D. Hayes, J. Fazo, T. Mitros, W. Dirks, U. Hellsten, N. Putnam, D.S. Rokhsar, Phytozome: a comparative platform for green plant genomics, Nucleic Acids Res. 40 (2012) D1178–D1186, https://doi.org/10.1093/nar/gkr944.
[28] H. Nielsen, Predicting secretory proteins with SignalP, Methods Mol. Biol. 1611 (2017) 59–73, https://doi.org/10.1007/978-1-4939-7015-5_6.
[29] E. Gasteiger, C. Hoogland, A. Gattiker, S. Duvaud, M.R. Wilkins, R.D. Appel, A. Bairoch, Protein identification and analysis tools on the ExPASy server, Proteomics Protoc. Handb, Humana Press, Totowa, NJ, 2005, pp. 571–607, , https://doi.org/10.1385/1-59259-890-0:571.
[30] S.F. Altschul, T.L. Madden, A.A. Schäffer, J. Zhang, Z. Zhang, W. Miller, D.J. Lipman, Gapped BLAST and PSI-BLAST: a new generation of protein database search programs, Nucleic Acids Res. 25 (1997) 3389, https://doi.org/10.1093/nar/25.17.3389.
[31] F. Corpet, Multiple sequence alignment with hierarchical clustering, Nucleic Acids Res. 16 (1988) 10881–10890, https://doi.org/10.1093/nar/16.22.10881.
[32] J.F. Morrison, Kinetics of the reversible inhibition of enzyme-catalysed reactions by tight-binding inhibitors, BBA - Enzymol. 185 (1969) 269–286, https://doi.org/10.1016/0005-2744(69)90420-3.
[33] G. Ren, Q. Tian, Y. An, B. Feng, Y. Lu, J. Liang, K. Li, Y. Shang, Y. Nie, X. Wang, D. Fan, Coronin 3 promotes gastric cancer metastasis via the up-regulation of MMP-9 and cathepsin K, Mol. Cancer. 11 (2012) 67, https://doi.org/10.1186/1476-4598-11-67.
[34] S.S. Cotrin, L. Puzer, W.A. De Souza Judice, L. Juliano, A.K. Carmona, M.A. Juliano, Positional-scanning combinatorial libraries of fluorescence resonance energy transfer peptides to define substrate specificity of carboxydipeptidases: Assays with human cathepsin, B, Anal. Biochem. 335 (2004) 244–252, https://doi.org/10.1016/j.ab.2004.09.012.
[35] J.O. Westgard, P.L. Barry, M.R. Hunt, T. Groth, A multi-rule Shewhart chart for quality control in clinical chemistry, Clin. Chem. 27 (1981) http://clinchem.aaccjnls.org/content/27/3/493.long.
[36] A.A. Siddiqui, P.S.S. Khaki, A. Sohail, T. Sarwar, B. Bano, Isolation and purification of phytocystatin from almond: Biochemical, biophysical, and immunological characterization, Cogent Biol. 2 (2016), https://doi.org/10.1080/23312025.2016.1262489.
[37] D. Musil, D. Zucic, D. Turk, R.A. Engh, I. Mayr, R. Huber, T. Popovic, V. Turk, T. Towatari, N. Katunuma, E. Al, The refined 2.15 A X-ray crystal structure of human liver cathepsin B: the structural basis for its specificity, EMBO J. 10 (1991) 2321–2330, https://doi.org/10.1002/j.1460-2075.1991.tb07771.x.
[38] Paulo C. Almeida, Iseli L. Nantes, Jair R. Chagas, Cláudia C.A. Rizzi, Adelaide Faljoni-Alario, Euridice Carmona, Luiz Juliano, Helena B. Nader, Ivarne L.S. Tersariol, Cathepsin B Activity Regulation: Heparin-like glycosaminoglycans protect human cathepsin B from alkaline pH-induced inactivation, J. Biol. Chem. 276 (2) (2001) 944–951, https://doi.org/10.1074/jbc.M003820200.
[39] C. Illy, O. Quraishi, J. Wang, E. Purisima, T. Vernet, J.S. Mort, Role of the occluding loop in cathepsin B activity, J. Biol. Chem. 272 (1997) 1197–1202, https://doi.org/10.1074/jbc.272.2.1197.
[40] D.K. Nägler, A.C. Storer, F.C.V. Portaro, E. Carmona, A. Luiz Juliano ‡, Robert Ménard*, Major increase in endopeptidase activity of human cathepsin b upon removal of occluding loop contacts†, Biochemistry 36 (1997) 12608–12615, https://doi.org/10.1021/bi971264.
[41] F. Strålberg, A. Kassem, F. Kasprzykowski, M. Abrahamson, A. Grubb, C. Lindholm, U.H. Lerner, Inhibition of lipopolysaccharide-induced osteoclast formation and bone resorption in vitro and in vivo by cysteine proteinase inhibitors, J. Leukoc. Biol. 101 (2017) 1233–1243, https://doi.org/10.1189/jlb.3A1016-433R.
[42] F. Strålberg, P. Henning, I. Gjertsson, B. Kindlund, P.P.C. Souza, E. Persson, M. Abrahamson, F. Kasprzykowski, A. Grubb, U.H. Lerner, Cysteine proteinase

inhibitors regulate human and mouse osteoclastogenesis by interfering with RANK signaling, FASEB J. 27 (2013) 2687–2701, https://doi.org/10.1096/fj.12-211748.
[43] M. Brage, A. Lie, M. Ransjö, F. Kasprzykowski, R. Kasprzykowska, M. Abrahamson, A. Grubb, U.H. Lerner, Osteoclastogenesis is decreased by cysteine proteinase inhibitors, Bone 34 (2004) 412–424, https://doi.org/10.1016/j.bone.2003.11.018.
[44] G. Huet, R.M. Flipo, C. Colin, A. Janin, B. Hemon, M. Collyn-d'Hooghe, R. Lafyatis, B. Duquesnoy, P. Degand, Stimulation of the secretion of latent cysteine proteinase activity by tumor necrosis factor alpha and interleukin-1, Arthritis Rheum. 36 (1993) 772–780, https://doi.org/10.1002/art.1780360606.
[45] R. Lemaire, G. Huet, F. Zerimech, G. Grard, C. Fontaine, B. Duquesnoy, R.M. Flipo, Selective induction of the secretion of cathepsins B and L by cytokines in synovial fibroblast-like cells, Br. J. Rheumatol. 36 (1997) 735–743, https://doi.org/10.1093/rheumatology/36.7.735.
[46] Q. Wang, Y. Zhang, J.P. Hall, L.L. Lin, U. Raut, N. Mollova, N. Green, J. Cuozzo, S. Chesley, X. Xu, J.I. Levin, V.S. Patel, A rat pharmacokinetic/pharmacodynamic model for assessment of lipopolysaccharide-induced tumor necrosis factor-alpha production, J. Pharmacol. Toxicol. Methods 56 (2007) 67–71, https://doi.org/10.1016/j.vascn.2007.02.001.
[47] R. Ruppert, E. Hoffmann, W. Sebald, Human bone morphogenetic protein 2 contains a heparin-binding site which modifies its biological activity, Eur. J. Biochem. 237 (1996) 295–302, https://doi.org/10.1111/j.1432-1033.1996.0295n.x.
[48] X. Wu, W. Shi, X. Cao, Multiplicity of BMP signaling in skeletal development, Ann. N.Y. Acad. Sci. 1116 (2007) 29–49, https://doi.org/10.1196/annals.1402.053.
[49] K. Fuller, K.M. Lawrence, J.L. Ross, U.B. Grabowska, M. Shiroo, B. Samuelsson, T.J. Chambers, Cathepsin K inhibitors prevent matrix-derived growth factor degradation by human osteoclasts, Bone. 42 (2008) 200–211, https://doi.org/10.1016/j.bone.2007.09.044.
[50] T. Komori, Regulation of bone development and extracellular matrix protein genes by RUNX2, Cell Tissue Res. 339 (2010) 189–195, https://doi.org/10.1007/s00441-009-0832-8.
[51] A. Bakopoulou, G. Leyhausen, J. Volk, A. Tsiftsoglou, P. Garefis, P. Koidis, W. Geurtsen, Comparative analysis of in vitro osteo/odontogenic differentiation potential of human dental pulp stem cells (DPSCs) and stem cells from the apical papilla (SCAP), Arch. Oral Biol. 56 (2011) 709–721, https://doi.org/10.1016/j.archoralbio.2010.12.008.
[52] B. Seshi, S. Kumar, D. Sellers, Human bone marrow stromal cell: coexpression of markers specific for multiple mesenchymal cell lineages, blood cells, Mol. Dis. 26 (2000) 234–246, https://doi.org/10.1006/BCMD.2000.0301.
[53] S.Z. Khan, E. Kokubu, K. Matsuzaka, T. Inoue, Behaviour of rat-cultured dental pulp cells in three-dimensional collagen type-1 gel *in vitro* and *in vivo*, Aust. Endod. J. 39 (2013) 137–145, https://doi.org/10.1111/j.1747-4477.2012.00351.x.
[54] B.-N. Lee, S.-J. Chun, H.-S. Chang, Y.-C. Hwang, I.-N. Hwang, W.-M. Oh, Physical properties and biological effects of mineral trioxide aggregate mixed with methylcellulose and calcium chloride, J. Appl. Oral Sci. 25 (2017) 680–688, https://doi.org/10.1590/1678-7757-2017-0050.
[55] H.-S. Lee, E.-Y. Jung, S.H. Bae, K.H. Kwon, J.-M. Kim, H.J. Suh, Stimulation of osteoblastic differentiation and mineralization in MC3T3-E1 cells by yeast hydrolysate, Phyther. Res. 25 (2011) 716–723, https://doi.org/10.1002/ptr.3328.
[56] L.F. Cooper, C.T. Harris, S.P. Bruder, R. Kowalski, S. Kadiyala, Incipient analysis of mesenchymal stem-cell-derived osteogenesis, J. Dent. Res. 80 (2001) 314–320, https://doi.org/10.1177/00220345010800010401.
[57] C.A. Gregory, W. Grady Gunn, A. Peister, D.J. Prockop, An Alizarin red-based assay of mineralization by adherent cells in culture: comparison with cetylpyridinium chloride extraction, Anal. Biochem. 329 (2004) 77–84, https://doi.org/10.1016/J.AB.2004.02.002.